THE DEVELOPMENT OF SURFACE VORTICES IN STRONGLY ROTATING FLOW IN A CYLINDRICAL VESSEL: NUMERICAL SIMULATION

F. Bloemeling
TUEV NORD NUCLEAR c/o TUEV NORD SysTec GmbH & Co. KG
Grosse Bahnstrasse 31, Hamburg, D-22525, Germany
fbloemeling@tuev-nord.de

S. Richter and M. Schlueter
Institute of Multiphase Flows
Hamburg University of Technology
Eissendorfer Strasse 38, Hamburg, D-21073, Germany
steffen.richter@tu-harburg.de

ABSTRACT

In many industrial applications, e.g. the emergency core cooling in nuclear power plants, the reliable operation of pumps is an indispensable requirement which can only be guaranteed when gas entrainment into the pumps is avoided. One of the main sources of gas entrainment are surface vortices which may develop at surfaces between a liquid and a gas if the liquid level is below a critical submergence of the pump intake. Thus, the determination of the critical submergence is a safety relevant matter for the design of pump intakes. Therefore, a test facility was built at the Hamburg University of Technology which provides experimental data on the shape of surface vortices in vertical vessels and strongly rotating flow. In this paper CFD results are presented concerning these experiments. The CFD simulations include a single phase approach as well as free surface simulations. To obtain the surface deformation in the single phase case the corresponding simulations are combined with an analytical vortex model whose applicability is discussed. The results from the single phase and the free surface simulations are then compared with each other and the experiment in order to assess the efficiency of the different strategies to compute the shape of surface vortices.

KEYWORDS

surface vortices, necessary submergence, CFD simulations, Burgers-Rott model, surface deformation

1. INTRODUCTION

An insufficient submergence of pump intakes leads to vortex formation at the water surface. Moreover, disturbances and nonsymmetries in the inflow cause swirling vortices, which require a significantly higher submergence [1] than vortex free inflows. These surface vortices have a strong negative influence on the pump behavior. Their swirl leads to disadvantageous inflow conditions at the impeller and induces vibrations, increased rotor loads and fluctuations in the pump behavior. Moreover, swirling surface vortices are characterized by strong gradients and large velocities in the vicinity of their center. Strong surface deformations and the development of a gas core are possible consequences. When the gas core reaches the pump, the entrained gas may lead to massive limitations or even the collapse of the pump flow rate [2]. Consequently, the formation of surface vortices at pump intakes must be avoided for a reliable pump operation.

The most efficient measure to avoid the mentioned problems is a sufficient submergence of the intake. Therefore, knowing the critical submergences of the intakes in the reservoir tanks and the pump sump is a relevant boundary condition for reactor safety analyses for Light Water Reactors, because it affects the available emergency cooling water during accidents.

The research alliance SAVE [3] has been initiated to investigate the conditions of surface vortex formation near pump intakes and the impact of gas entrainment on pumps and valves. The project includes experimental measurements with modern measurement techniques like, e.g. High-Speed Particle Image Velocimetry, Gamma and X-ray Tomography as well as numerical simulations.

To investigate the influence of different flow conditions and the influence of the shape of the intake on the development of surface vortices experiments are performed first in a down-scaled cylindrical vessel. In these experiments the velocity field in the vessel and the shape of the occurring surface vortices are measured. These measurements are used to validate corresponding CFD simulations and to set up experiments in a larger vessel of industrial scale. Furthermore, scaling effects can be examined by comparing the measurements in both vessels.

There are already several successful attempts by other researchers to compute the shape of surface vortices by means of CFD simulations. Particularly, the volume of fluid method turned out to be a suitable candidate (see e.g. [4], [5]). Although, this method is computationally intensive. Therefore, in the SAVE project we are seeking for a more efficient alternative. In this regard the combination of single phase CFD simulations and analytical vortex models like the Burgers-Rott model is a promising approach. This statement is based on the observation that a satisfying CFD quality can be achieved outside the vortex core with comparably small effort. Hence, the analytical model is only used to describe the flow field inside the vortex core and the required information to complete the analytical model is extracted from the CFD data. This has been done before by other authors (e.g. [6]), but the method which is applied here is a universal approach (it does not depend on the knowledge of case specific data) and differs slightly from other methods (more details can be found in [12]). However, at the beginning it wasn’t clear whether the Burgers-Rott model can be applied at all, because in contrast to other experiments the experiments performed at the Hamburg University of Technology aren’t rotationally symmetric. Therefore, first it must be checked whether elementary requirements of the Burgers-Rott model are fulfilled. The corresponding results are presented in this paper. Then the vortex shapes which are computed via the combination of single phase simulations and the Burgers-Rott model are compared with the experimental data and also with two phase CFD simulations. The latter ones make use of a two fluid approach rather than the volume of fluid method, because another future goal is to quantify the entrained air. This will require the consideration of dispersed flow and therefore the two fluid method has the advantage that it is not necessary to resolve the surface of every single bubble like it would be the case when interface capturing methods are used.

2. THE SCALED TUHH EXPERIMENTS

A particular focus of the research alliance SAVE is set on the conditions under which surface vortices occur near pump intakes and on the shape of those vortices. For the analysis of these parameters a large test facility has been built at the Hamburg University of Technology (TUHH). It consists of a large cylindrical vessel in original plant scale (Fig. 1). A vertical pump intake is located at its bottom and water is pumped into the cylinder through four adjustable pipes. Furthermore, the orientation of these pipes imposes a circulation on the flow in the test vessel.

Figure 1. TUHH test vessel (D=4 m)

Because the experiments in the large scale vessel are quite elaborate a smaller version in lab scale has been built which is used for pretesting (Fig. 2). In contrast to its large counterpart the down-scaled vessel is made from Plexiglas. Thus, optical measurements like High Speed Particle Image Velocimetry (HPIV) are much easier to perform. Furthermore, geometry changes can be realized with only small effort. For this reason, also the influence of different intake geometries is tested mainly in the scaled experiments.

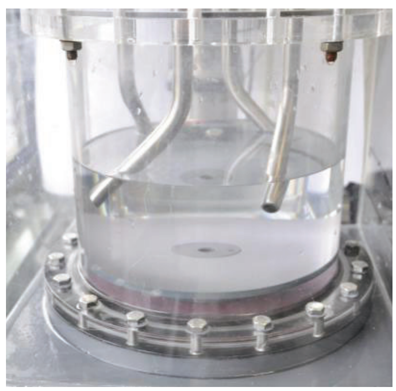

Figure 2. Scaled TUHH experiment

In the work which is presented in this paper a bell mouthed intake was used whose diameter is two times the pipe diameter. The intake pipe and the four inlet pipes have an inner diameter of 15 mm each. The vessel has a diameter of 290 mm and is filled with water up to a level of 110 mm. To ensure a constant water level the piping system is a closed circuit. Water leaves the vessel through the intake and it is pumped back through the four inlet pipes. The inlet pipes are immersed and cross the water surface in a 45° angle. Moreover, to impose a circulation their orientation is not outwards. Instead they form another 45° angle with the radial direction.

Depending on the volume flow rate different types of surface vortices can be observed. They can be classified in six groups shown in Fig. 3. The first type shows no surface deformations. The occurrence of small dips characterizes vortices of type two. The transition from type one to type two occurs at the critical submergence. If the vortex core can be made visible with dye, vortex type three is reached. Types four and five are characterized by the fact that small particles or bubbles are entrained by the vortex, respectively. A surface vortex with a fully developed gas core which reaches from the surface to the intake is type six. In general, vortices of type three or higher should be avoided in industrial applications.

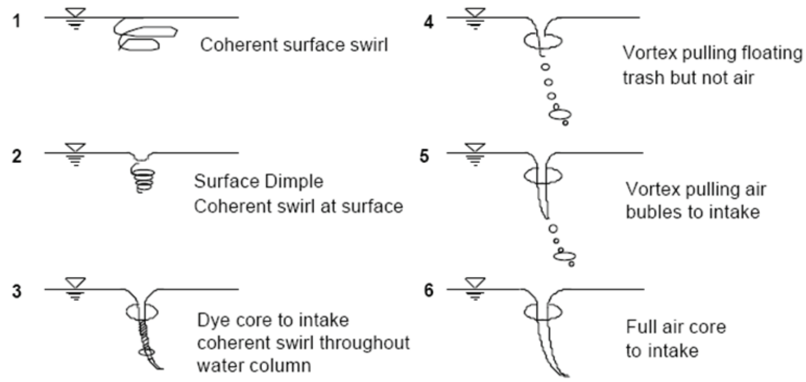

Figure 3. Types of surface vortices [1]

During the experiment in question water is pumped through the test section with a constant mass flow rate of 0.0694 kg/s. That leads to a surface vortex with a distinct gas core. But the gas core doesn't reach the intake. So it is either type three or four. Measurements took place by taking photographs of the gas core. The observed gas core length was 67±9 mm.

3. CFD MODEL

3.1. General

To exploit the symmetric setup only a quarter of the vessel has been modeled. Therefore, only one inlet pipe is contained in the geometry and at the two vertical cut planes periodic boundary conditions are set. Furthermore, it is not necessary to model the entire water circuit. Hence, the outlet is placed 67.5 mm downstream the intake. The other boundary conditions and also the grids depend on whether it is a single phase or a free surface simulation.

3.2. Single Phase Model

A single phase CFD simulation is a common choice for the analysis of surface vortices because it avoids the large immanent effort of two phase simulations. In this context single phase means that only the liquid phase (here: water) is considered. Instead of modeling a free surface between water and air, a free slip wall is placed on top of the water. As a consequence of an unmovable wall at the top some error in the pressure distribution has to be accepted. And obviously no kind of surface deformation can be handled without some additional effort.

The water is modeled as incompressible liquid and the material properties correspond to atmospheric conditions. To consider the effect of turbulence the shear stress transport model [7] (SST model) has been chosen with automatic wall treatment. Automatic wall treatment allows switching between a wall function formulation and a low-Re model automatically. However, since two equation models like the SST model have deficiencies related to strongly rotating flows, an algebraic curvature correction [8] was added which considers the anisotropic character of strongly rotating flows.

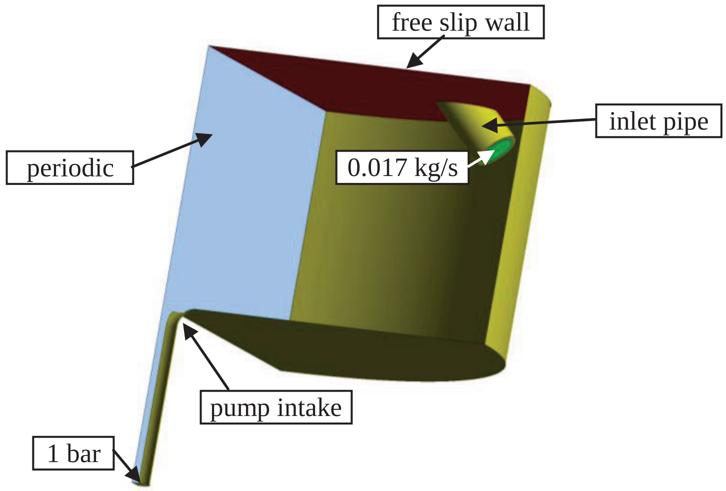

Figure 4. Single phase CFD model with boundary conditions

Therefore, the underlying equations for the single phase model are the Reynolds Averaged Navier-Stokes equations (RANS) for incompressible flow.

$$\rho_w \frac{\partial u_w}{\partial t} + \rho_w \, u_w \cdot \nabla u_w = -\nabla p + \mu_w \, \Delta \, u_w + \nabla \cdot (S_t) + f \, , \tag{1}$$

$$\nabla \cdot u_w = 0 \tag{2}$$

In the above equations ρ_w is the water density, u_w denotes the water velocity and μ_w its viscosity. Furthermore, S_t is the Reynolds stress tensor and f is a body force (here: gravity).

An inlet boundary condition is placed at the opening of the inlet pipe. A mass flow rate of 0.017 kg/s is prescribed at this inlet. At the outlet downstream the pump intake a pressure condition of 1 bar is set. Strictly speaking, this doesn't match the experiment exactly, because actually the pressure at the water surface is 1 bar. But this is no relevant restriction, since it leads only to a slight shift in the absolute pressure. The geometry and the boundary conditions are shown in Fig. 4. A detailed description of the grids is given in chapter 4.2. which contains a grid study.

3.3. Free Surface Model

To decide whether it is necessary to model the surface between water and air exactly, a free surface model of the experiment was set up, too. First of all that implies that two phases -water and air- and their interactions have to be modeled. To ensure a sufficient distance of the boundary conditions from the water surface the geometry model was extended by an air domain on top of the water (see Fig. 5).

Since compressibility effects of the air are not expected to play any significant role, the air is modeled with constant material properties. Furthermore, both liquids are assumed to be continuous phases in an Euler-Euler context. To be more specific, the basic transport equations for mass and momentum are formulated as a two fluid model [9] which means that every liquid has its own set of equations involving the volume fraction of the specific liquid. For instance the momentum equation for the water phase can be written as

$$\frac{\partial}{\partial t}(\alpha_w \, \rho_w \, u_w) + \nabla \cdot (\alpha_w \, \rho_w \, (u_w \otimes u_w)) = -\alpha_w \nabla p + \nabla \cdot (\alpha_w \, (S_v + S_t)) + \alpha_w f + \Phi \tag{3}$$

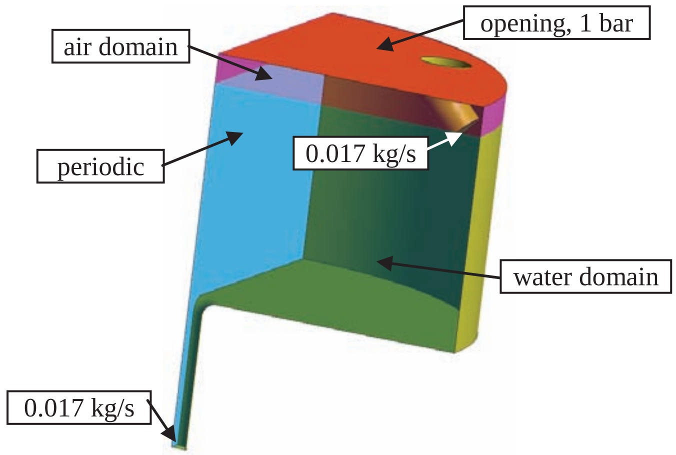

Figure 5. Free surface CFD model with boundary conditions

Here, the volume fraction of water is denoted by α_w and the viscous and turbulent stresses are S_v and S_t, respectively. The term Φ refers to the transfer of momentum between both phases.

The idea of the two fluid approach is that a computational cell may contain both phases at the same time. The volume fraction of the phase specifies which fraction of the cell is occupied by the phase. Mathematically speaking, the governing equations are the result of an averaging operation applied to the original transport equations for mass and momentum (eq. (1) and (2)). For more details about the two fluid model we refer to the book of Ishii [9].

However, Merzari et al. [5] and Ito et al. [4] successfully applied the volume of fluid method to compute the shape of surface vortices. Nevertheless, the two fluid model has been chosen for this study, because in principle it offers simulating the deformation of the free surface and dispersed flow without resolving the exact shape of every single bubble. Although this is not subject of this paper, treating dispersed bubbles will be necessary to quantify air entrainment in future simulations.

Therefore, due to the two fluid method one doesn't have to account for the exact shape of the interphase between the two liquids. Thus, it is not necessary to deal with complex discontinuities. But for the same reason information concerning the interaction of the phases is lost. Therefore, the transfer of mass and momentum has to be modeled.

Since there is no mass transfer between water and air in the experiment, only the momentum transfer term Φ has to be considered. The dominant contribution to the momentum transfer comes from the drag force. Moreover, due to large density differences the water rather influences the air than vice versa. Therefore, for the gaseous phase the water behaves like a solid. Hence, Newton' s drag law, which postulates that inertia forces dominate the viscous forces, can be applied:

$$\Phi = 0.44\, \rho_m\, a \left\| u_a - u_w \right\| \left(u_a - u_w \right), \qquad (4)$$
$$\rho_m = \alpha_w\, \rho_w + \left(1 - \alpha_w\right) \rho_a$$

In equation (4) ρ_a and u_a denote the density and the velocity of air, respectively. The interfacial area density a which describes the amount of interfacial area per unit volume is computed via

$$a = \left\| \nabla \alpha_w \right\| \qquad (5)$$

Again the SST model with curvature correction is used as turbulence model for both phases.

The boundary conditions differ from the single phase case because the pressure condition of 1 bar is set to the top of the air domain. Furthermore, an opening boundary condition was chosen at this place to allow the air to enter and to leave the vessel. The vertical circumference of the vessel is again a no-slip wall. Moreover, the inlet and outlet conditions have changed. Only water is allowed to enter the vessel through the inlet pipes and to leave the test section through the intake. At both places a bulk mass flow rate of 0.017 kg/s is prescribed. Details about the meshing of the free surface model are given in chapter 4.2.

4. NUMERICAL RESULTS

4.1. General remarks

All numerical computations were performed with ANSYS CFX 15 [10]. CFX uses a finite volume method to discretize the continuous transport equations. In short, that means the transport equations are transformed to an integral representation for every computational cell. This method has the advantage that conservation of the transport properties can be achieved easily. But their values and fluxes at the cell boundaries have to be approximated numerically [11].

For the advection terms the High Resolution scheme was used which is a higher order method that uses flux limiters to limit the total variation of the solution [10]. Only in case of the turbulence properties (turbulent kinetic energy, specific dissipation rate) the Upwind method was used. The transient terms were discretized by an implicit second order Euler approach. For more details about the numerical methods provided by CFX the interested reader is referred to the manual [10].

In the following several single phase as well as multi phase simulations are presented that pursue different objectives. Chapter 4.2. starts with a grid study to analyze the influence of the grid resolution on the simulation results. Then attention turns to the superordinate target which is the computation of the vortex shape that was observed in the experiment. Clearly, it is not possible to compute any surface deformation with the single phase approach. But it is possible to combine the CFD results with an analytical vortex model which then yields the surface deformation [12]. For this purpose the applicability of the analytical vortex model of Burgers and Rott is investigated in chapter 4.3. In the succeeding chapter 4.4. the shape of the gas core is computed in two ways. In case of the single phase simulations it is computed by means of the analytical vortex model and in case of the free surface simulations CFX itself provides the deformation of the water surface. Furthermore, both methods are compared to the experimental measurements. The comparisons in chapter 4.4. serve also another purpose. They shall answer the question, whether it is necessary to perform free surface calculations to obtain the correct surface deformation or not. In addition it shall be analyzed whether a transient calculation yields the same results as its stationary counterparts.

4.2. Grid study

Grid studies are in general obligatory for the generation of reliable CFD results [13]. Without testing the influence of the grid resolution on the simulation results it is difficult to assess the discretization error of the simulation. For this reason three different grids were generated. Grid one is the coarsest grid and grid two emanates from a uniform refinement of the first one by a factor of 1.2 in every spatial direction. A second refinement by the same factor yields grid three. The wall resolution is the same for all three grids, because it turned out to be fine enough for our purposes. Since all grids look very similar only grid one is displayed in Fig. 6.

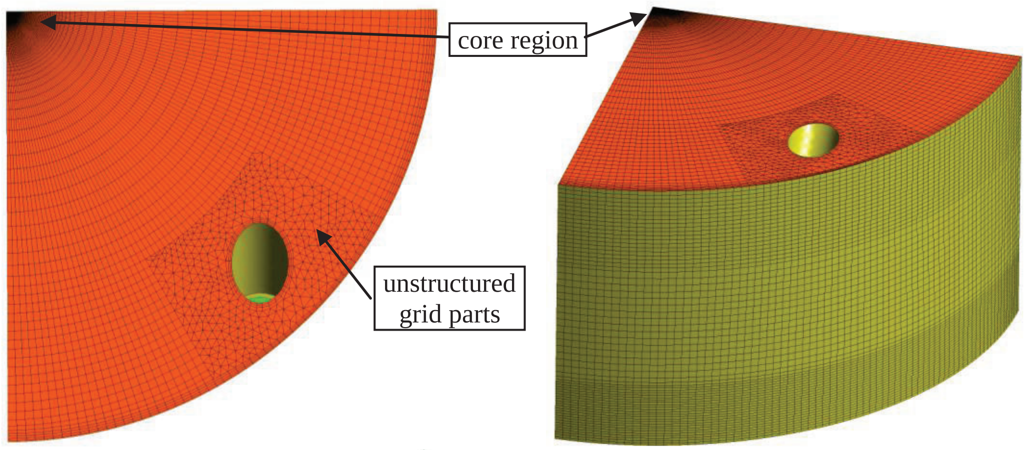

Figure 6. Grid 1

The grids consist mainly of hexahedral elements which are as much aligned with the flow as possible. The only exception is the region near the inlet pipe. Because of the inclination of the inlet pipe an unstructured meshing technique with tetrahedral elements yields higher grid qualities. The two grid types are connected with pyramids. The finest grid parts are located in the vessel center where the vortex occurs. This is necessary to resolve the surface vortex. The most important grid parameters are summarized in table I.

Table I. Grid statistics

Grid	Elements	Max. element size	Core region resolution (horizontal)
1	903,892	3 mm	0.08 mm
2	1,687,929	2.4 mm	0.06 mm
3	3,135,344	1.9 mm	0.05 mm

Plots of the azimuthal velocity components in cylindrical coordinates along a horizontal line (line 1, see also Fig. 10) are shown for all three grids in Fig. 7. The axial distance of the line to the intake is 110 mm. So the line is at the water surface. The graphs corresponding to the three grids nearly coincide. This is particularly true in the region outside the vortex core. But also inside the vortex core the graphs match quite well. So no significantly different results are expected from further refinements at least in the single phase case.

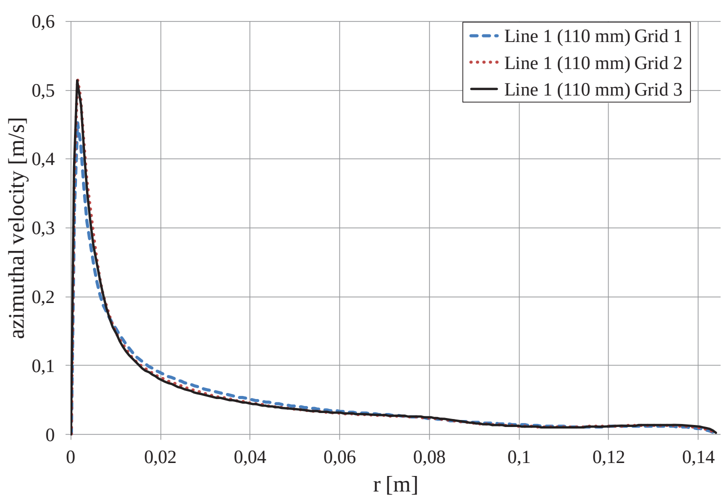

Figure 7. Comparison of azimuthal velocities

For the free surface simulations an air domain has been placed above the water which has to be meshed, too. Furthermore, the air/water interface needs some special treatment. The starting basis for grid four is grid 1. Grid 1 was extended by a few layers of hexahedral elements at the top. These layers become denser at the initial water level and were extruded to form the grid of the air domain (see Fig. 8).

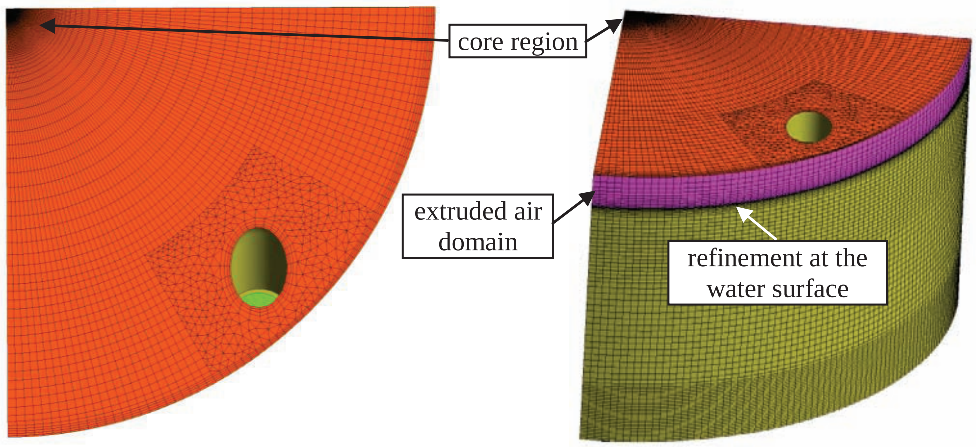

Figure 8. Grid 4

Grid 1 has been chosen, because it already produces very similar results than the other grids (cmp. Fig. 7). However, this assessment is based on single phase simulations and it doesn't need to be true for the free surface simulations. The reason is that the surface of the gas core has a strong curvature. The exact reproduction of this curved surface might have stronger requirements regarding the grid resolution than a single phase simulation. This hasn't been checked yet. The statistics of grid four are summarized in table II.

Table II. Properties of grid 4

Grid	Elements	Max. element size	Core region resolution (horizontal)
4	1,060,533	3 mm	0.08 mm

4.3. Comparison with the Burgers-Rott model

Burgers and Rott developed an analytical vortex model which is based on the assumption of rotating stagnation flow [14]. They assumed the following radial and axial velocity field

$$u_r = -\frac{1}{2}\kappa\, r, \tag{6}$$

$$u_z = \kappa\, z \tag{7}$$

and by substituting the above equations into the Navier-Stokes equations they obtained

$$u_\phi = \frac{\Gamma_\infty}{2\pi r}\left[1 - exp\left(-\frac{r^2}{4\nu/\kappa}\right)\right] \tag{8}$$

for the azimuthal velocity component. The variables r and z describe the radial and axial coordinate and ν denotes the kinematic viscosity. Furthermore, this model depends on two parameters, the so-called suction parameter κ and the circulation Γ_∞. The circulation is defined by the curve integral along a closed curve C which encloses the vortex.

$$\Gamma = \oint_C \vec{u} ds \tag{9}$$

In the case of axisymmetric potential flow the circulation is constant and can be expressed by $\Gamma = 2\,\pi\, r\, u_\phi$ which leads directly to the vortex model of Rankine. Both parameters, the suction parameter and the circulation as well, can be determined from the CFD results (see also [12], [15]).

The water surface fulfills the pressure condition

$$p(h(r),r) = const. \quad \Leftrightarrow \quad \frac{dh}{dr} = -\left(\frac{\partial p}{\partial z}\right)^{-1} \frac{\partial p}{\partial r} \tag{10}$$

which allows the computation of the gas core shapes of surface vortices by using the Burgers-Rott model (eq. (6) – (8)) [6].

As already mentioned the Burgers-Rott model assumes axisymmetric and stationary flow. Moreover, it asymptotically approaches potential flow conditions outside the vortex core region. Thus, except in the core region of the vortex the flow should be irrotational. So during the rest of this chapter it will be checked whether the experimental flow conditions fulfill these assumptions. This investigation is based on the single phase CFD simulations with the finest grid three.

Since there are four inlet pipes the assumption of axisymmetric flow cannot be fulfilled globally. But Fig. 9 shows that the flow becomes axisymmetric when it approaches the intake. Fig. 9 displays a contour plot of the azimuthal velocity. Clearly, it isn't axisymmetric in the outer regions near the inlet pipes. But approaching the center of the vessel the contour lines become more and more circular. Thus, at least in the vicinity of the surface vortex there is axisymmetric flow. Hence, this requirement of the Burgers-Rott model is fulfilled locally.

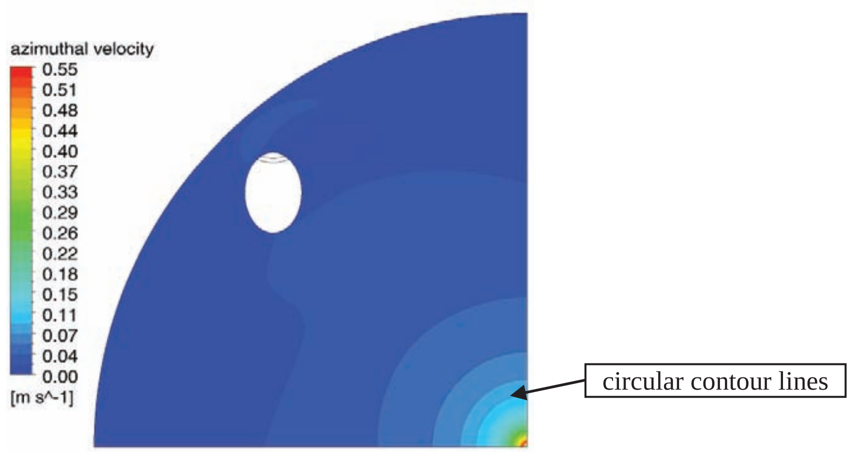

Figure 9. Azimuthal velocities at the surface

Another property of the Burgers-Rott model is that the azimuthal velocities are independent of the axial coordinate z. Again it cannot be expected that this assumption is true everywhere in the test vessel. But the graphs in Fig. 10 of the azimuthal velocities in three different levels (lines 1 to 3) show that it is fulfilled locally, too. The position of the corresponding lines is shown on the right side in Fig. 10. Near the center of the vessel there is basically no difference between the three graphs. The first deviations occur at a distance from the center larger than 40 mm.

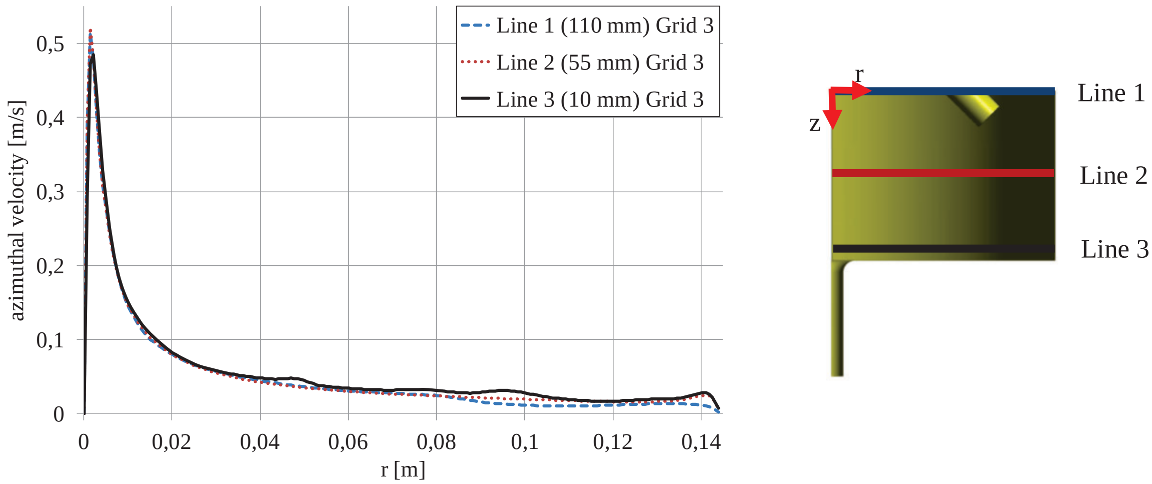

Figure 10. Azimuthal velocities in different heights

Due to the analytical vortex model the surface vortex can be split into a core region where the circulation behaves approximately linearly and a free vortex region with potential flow. In the latter region the circulation is constant. This behavior can be observed in Fig. 11, too. Outside the core region the circulation reaches a plateau of constant circulation (green region in Fig. 11). The value corresponding to the plateau is 0.0092 m²/s. At a distance of ca. 12 mm the circulation increases again. Therefore, the model is no longer valid. But the center part of the flow is very similar to the model.

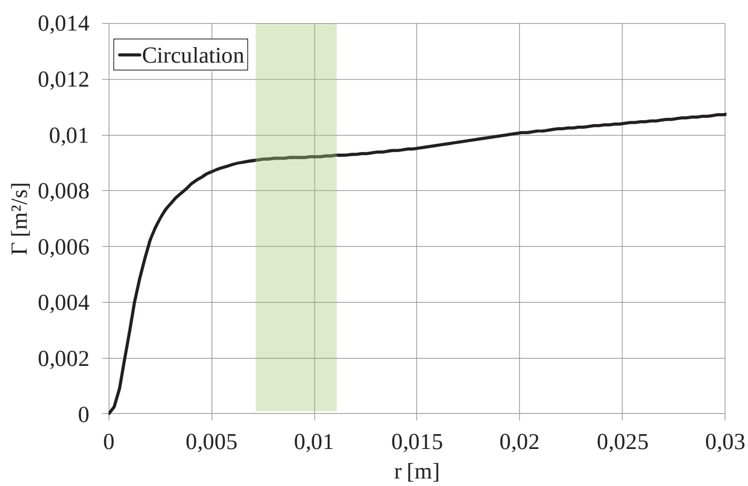

Figure 11. Circulation at the surface

So far it was possible to verify basic requirements of the Burgers-Rott model at least locally. But a look at the streamlines in Fig. 12 reveals that it is not a stationary flow regime. In the wake of the inlet pipes there is a clearly visible zone of vortex shedding. Therefore, it is not possible to obtain a fully converged stationary numerical solution. Instead the iterations showed an oscillatory behavior in an advanced stage of the solution process which seems to correlate with the vortex shedding frequency. The oscillations also affect the surface vortex in the middle. It periodically grows and shrinks. This behavior has been observed in the experiments, too. Therefore, there is a slight discrepancy compared to the assumptions of the Burgers-Rott model. However, it turned out that the Burgers-Rott model is still very useful if the flow is regarded as quasi-stationary and throughout the text CFD data were used in which the tangential velocities near the center reach a maximum.

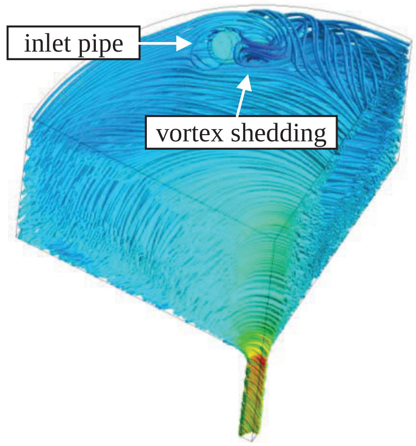

Figure 12. Streamlines in the test vessel

4.4. Gas cores

Since it has been shown in the preceding chapter that fundamental requirements for an application of the Burgers-Rott model are fulfilled in the center of the test vessel, it is apparent to use equation (10) for the computation of the surface deformation. Only two parameters have to be determined for that purpose, the circulation and the suction parameter. The value of the circulation in the free vortex region has already been determined as $\Gamma_\infty = 0.0092$ m²/s . An appropriate procedure to gain the suction parameter is described for instance in [15]. Following this approach the suction parameter takes the value 1.6 1/s. These parameters complete the Burgers-Rott model and equation (10) can be applied. A comparison between the computed surface deformation and the measured gas core length is shown in Fig. 13. The agreement between the computations and the experiment is very good. The computed gas core is exactly as long as in the experiment.

Things look different for the free surface simulations. Although the two phase simulations yield a distinct surface deformation (see Fig. 14), the comparison in Fig. 13 shows that it is much too small compared to the experimental data (dotted red curve in Fig. 13). In the CFX simulation the water surface is lowered by 10 mm. In contrast, the measured gas core length was about 67 mm. Therefore, it seems that a correct reproduction of the surface deformation with a free surface simulation requires a much finer grid resolution at least in the axial direction or some other model variations. However, the width of the surface vortex predicted by CFX is the same as the one computed with the Burgers-Rott model. And also the shapes of the vortices coincide near the vortex boundary. Therefore, in principle it seems to be possible to compute the exact shape of the surface vortex with the two fluid model if one is willing to accept the corresponding effort.

To dispel doubts that CFX underestimates the gas core length just because it was a stationary simulation also a transient simulation was carried out. But this didn't change the results. In the transient case CFX predicts a gas core length of 1 cm also which is still too small.

Hence, it turned out that the combination of single phase CFD simulations with the Burgers-Rott model is an efficient approach to predict the gas core lengths of surface vortices. The computation of the gas core lengths by means of free surface simulations requires much more effort. In fact, all simulations result in an underestimation of the gas core length, although evidence suggests that it can be possible to compute the exact length in principle. Also, a transient two phase simulation didn't remedy this situation. It didn't improve the results compared to its stationary counterpart.

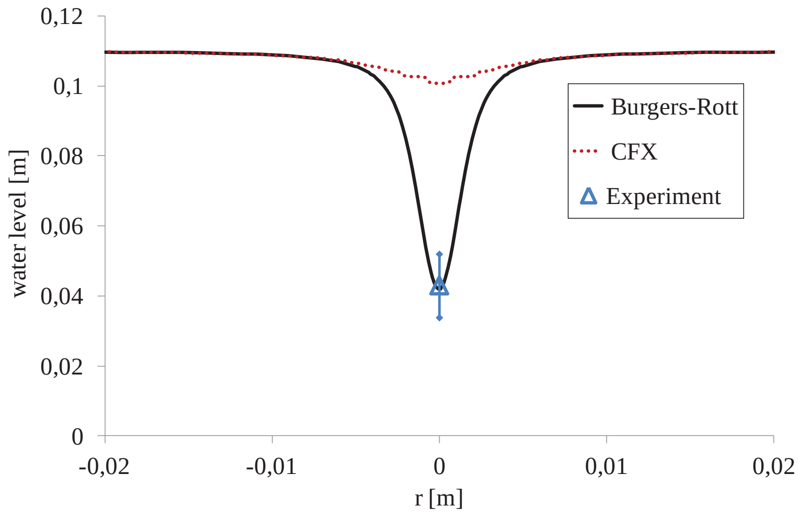

Figure 13. Computed water surface vs. experiment

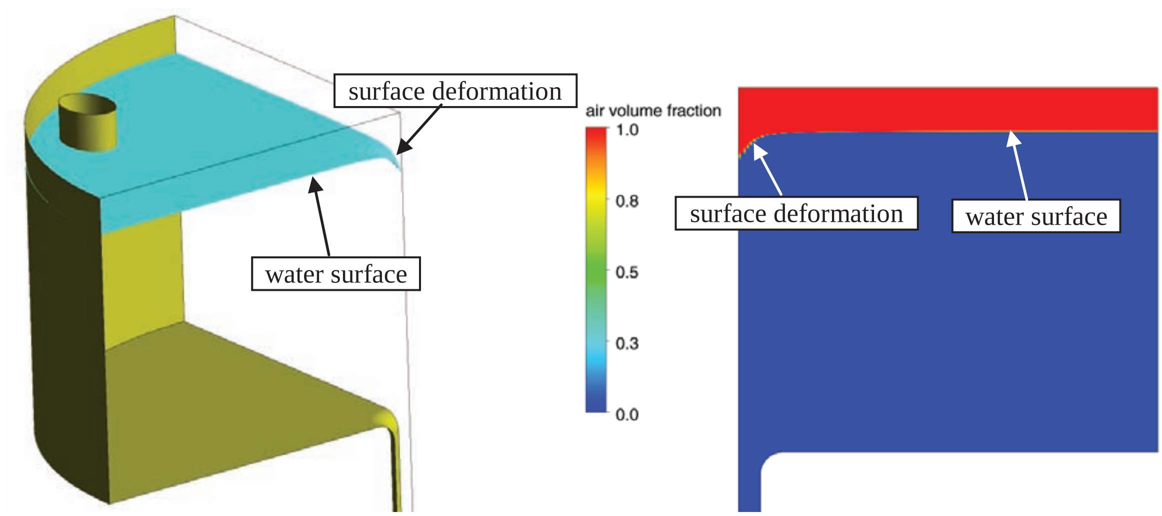

Figure 14. Surface deformation computed by CFX

The ability of the combined approach to forecast the gas core length of surface vortices can be utilized to determine also the critical submergence. Obviously, it is possible to check whether a given submergence suffices to avoid hollow surface vortices. Pandazis [12] has demonstrated how to use this methodology for an efficient computation of the critical submergence.

5. CONCLUSIONS

In order to analyze the development of surface vortices, an experiment in a scaled test vessel was carried out at the Hamburg University of Technology. Numerical simulations which correspond to this experiment were presented in this paper. Two different CFD models were applied during the simulations, a single phase and a free surface model. Since the single phase version doesn't provide any information of a surface deformation it was necessary to make use of the analytical vortex model of Burgers and Rott which allows the computation of the vortex shape. Therefore, in a first step the fulfillment of basic requirements of this model has been checked. It could be shown that nearly all requirements are fulfilled at least locally in the vicinity of the surface vortex. Thus, the combination of the analytical vortex model and the CFD result were used to compute the shape of the occurring surface vortex. The computed gas core length coincided very well with the experimental measurements. Compared to the single phase calculations the simulations with the free surface model required much more computational effort and it turned out that it didn't succeed to compute the correct shape of the water surface. Although it was possible to compute a distinct dimple, its gas core was much too small. Also a transient calculation didn't improve this result. Thus, it seems more efficient to combine the Burgers-Rott model with single phase CFD simulations provided that the requirements of the analytical model are fulfilled. This strategy produced very good results at a fraction of the necessary effort for the two phase simulations.

ACKNOWLEDGMENTS

This work is sponsored by the German Federal Ministry of Education and Research (BMBF) under the contract numbers 02NUK023A and 02NUK023C. The responsibility for the content of this publication lies with the author.

REFERENCES

1. J. Knauss, "Swirling Flow Problems at Intakes," *IAHR Hydraulic Structures Design Manual*, A. A. Balkema, Rotterdam, Netherlands (1987).
2. J. Weinerth, "Kennlinienverhalten und Rotorbelastung von axialen Kühlwasserpumpen unter Betriebsbedingungen," PhD thesis, TU Kaiserslautern, Germany (2003).
3. "Verbundprojekt SAVE: Sicherheitsrelevante Analyse des Verhaltens von Armaturen, Kreiselpumpen und Einlaufgeometrien unter Berücksichtigung störfallbedingter Belastungen," http://www.tuhh.de/save/willkommen.html (2015)
4. K. Ito, T. Kunugi, H. Ohshima, T. Kawamura, "Formulations and Validations of a High-Precision Volume-of-Fluid Algorithm on Nonorthogonal Meshes for Numerical Simulations of Gas Entrainment Phenomena," *Journal of Nuclear Science and Technology*, Vol. **46**(3), pp. 366-373 (2009)
5. E. Merzari, H. Ninokata, S. Wang, E. Baglietto, "Numerical Simulation of Free-Surface Vortices," *Nuclear Technology*, Vol **165**, pp. 313-320 (2009)
6. K. Ito, T. Sakai, Y. Eguchi, H. Monji, H. Ohshima, A. Uchibori, Y. Xu. "Improvement of Gas Entrainment Prediction Method, Introduction of Surface Tension Effect", *Journal of Nuclear Science and Technology*, **47**(9), pp. 771-778 (2010)
7. F. R. Menter, "Two-Equation Eddy-Viscosity Turbulence Models for Engineering Applications," *AIAA Journal*, **32**(8), August (1994)
8. P. E. Smirnov, F. R. Menter, "Sensitization of the SST Turbulence Model to Rotation and Curvature by Applying the Spalart-Shur Correction Term," ASME Paper GT 2008-50480, Berlin, Germany (2008)
9. M. Ishii, T. Hibiki, "Thermo-Fluid Dynamics of Two-Phase Flow", Springer (2006)
10. ANSYS Germany GmbH, *ANSYS CFX Users Manual*, http://de-de.ansys.com/de_de (2015)
11. J. H. Ferziger, M. Peric, *Computational Methods for Fluid Dynamic*, Springer-Verlag Berlin Heidelberg New York (2002)
12. P. Pandazis, F. Blömeling, "Investigation of the Critical Submergence at Pump Intakes Based on Multiphase CFD Calculations," *7th International Conference on Computational and Experimental Methods in Multiphase and Complex Flows*, A Coruna, Spain, July 3-5, 2013
13. Nuclear Energy Agency, "Best Practice Guidelines for the Use of CFD in Nuclear Reactor Safety Applications," NEA/CSNI/R(2007)5, May (2007)
14. N. Rott, "On the Viscous Core of a Line Vortex," *ZAMP*, **9**(5-6), pp. 543-553 (1958)
15. P. Pandazis, F. Blömeling, "Determination of the Critical Submergence of Pump Intakes in Large Scale Vessels," *2nd International Symposium on Multiscale Multiphase Process Engineering*, Hamburg, Germany, September 24-27, 2014